*Paleoceanography and Paleoclimatology*

Supporting Information for

# Orbital-scale global ocean sea surface temperatures coupling with cryosphere-carbon cycle changes over the past 4 million years

Ze Zhang[1], Eelco J. Rohling[2,3], David B. Kemp[4], Zhixiang Wang[5*], Chunju Huang[4*]

[1]Department of Atmospheric Science, School of Environmental Studies, China University of Geosciences, Wuhan 430074, China

[2]Department of Earth Sciences, Utrecht University, Princetonlaan 8, 3584 CB Utrecht, The Netherlands

[3]Ocean and Earth Science, University of Southampton, National Oceanography Centre, Southampton, SO14 3ZH, UK

[4]State Key Laboratory of Biogeology and Environmental Geology and Hubei Key Laboratory of Critical Zone Evolution, School of Earth Sciences, China University of Geosciences, Wuhan 430074, China

[5]Qinghai Provincial Key Laboratory of Geology and Environment of Salt Lakes, Qinghai Institute of Salt Lakes, Chinese Academy of Sciences, Xining 810008, China

## Contents of this file

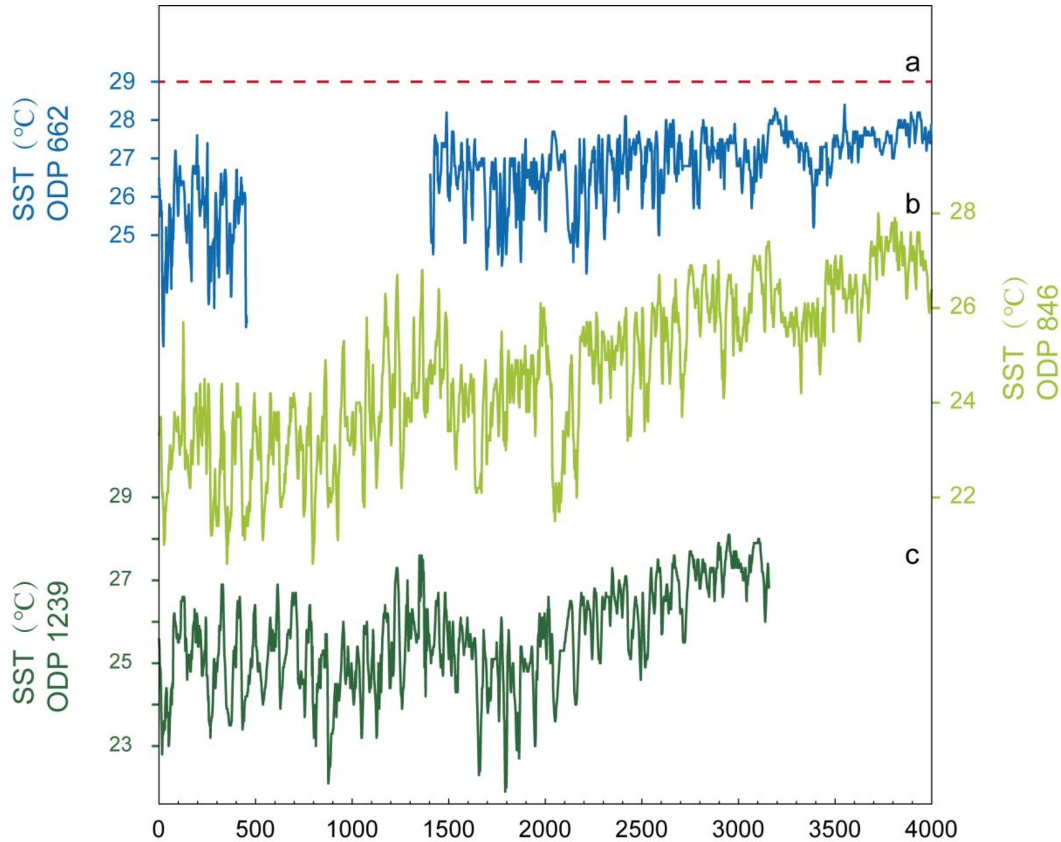


**Fig. S1. SST records from the tropics reconstructed by previous studies.** ODP Site 662 (1°S, 12°W; Herbert et al., 2010) from the equatorial Atlantic; ODP Site 846 (3°S, 91°W; Liu and Herbert, 2004; Lawrence et al., 2006) and ODP Site 1239 (1°S, 82°W; Etourneau et al. 2010) from the Equatorial Pacific. The dashed line is the threshold temperature of 29°C for reconstructing SSTs using the alkenone unsaturation index ($U^{K'}_{37}$; Li et al. 2011; Fedorov et al., 2013).

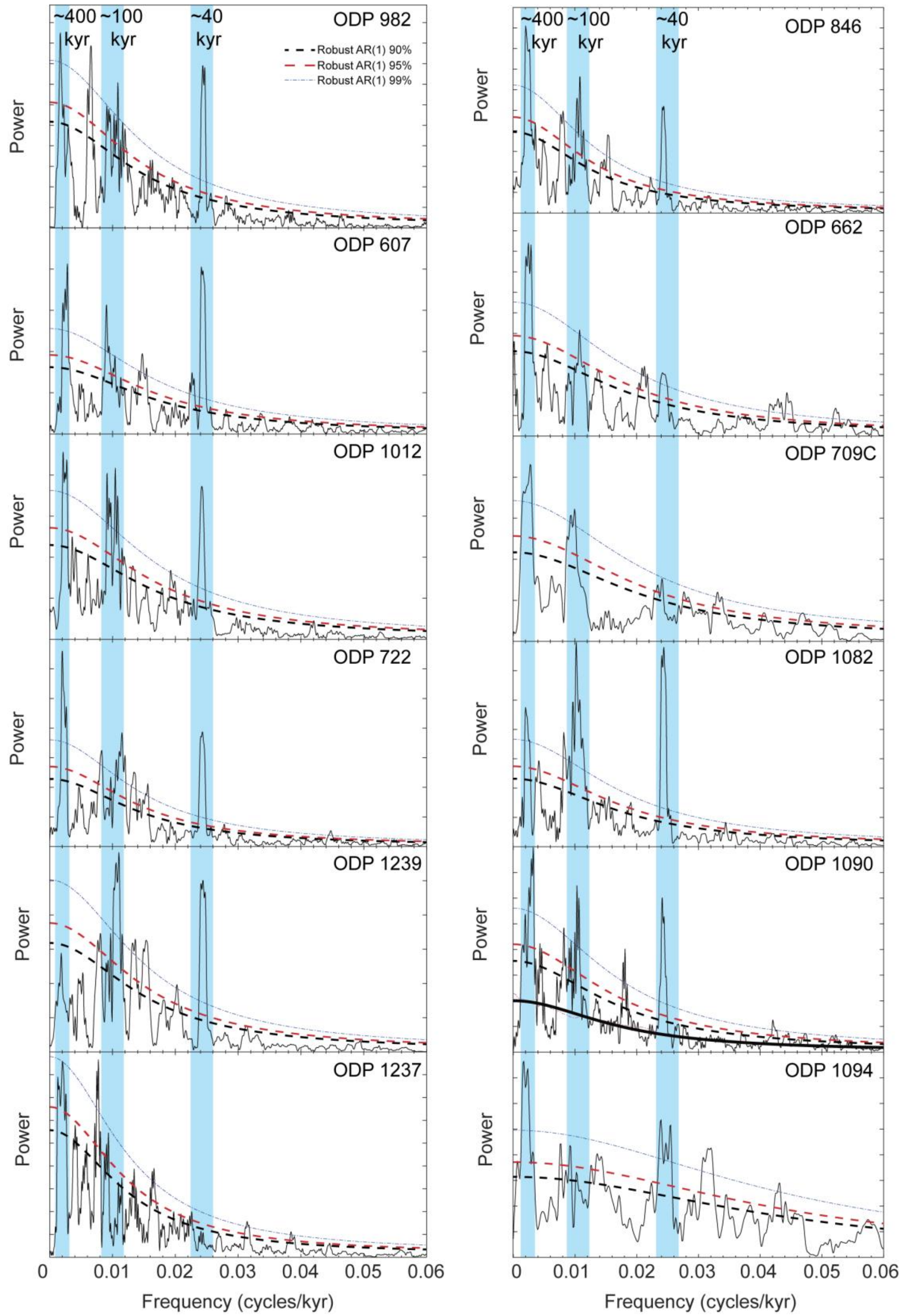


**Fig. S2 Spectral analysis of SSTs at each site.** All test data were detrended by removing 35% of the long trend using the LOESS functions. The SST spectra were analyzed using the 2π-MultiTaper Method (MTM) with robust red noise modeling used to ascertain the 90%, 95%, and 99% confidence levels of the spectra (black, red and blue dotted lines, respectively).

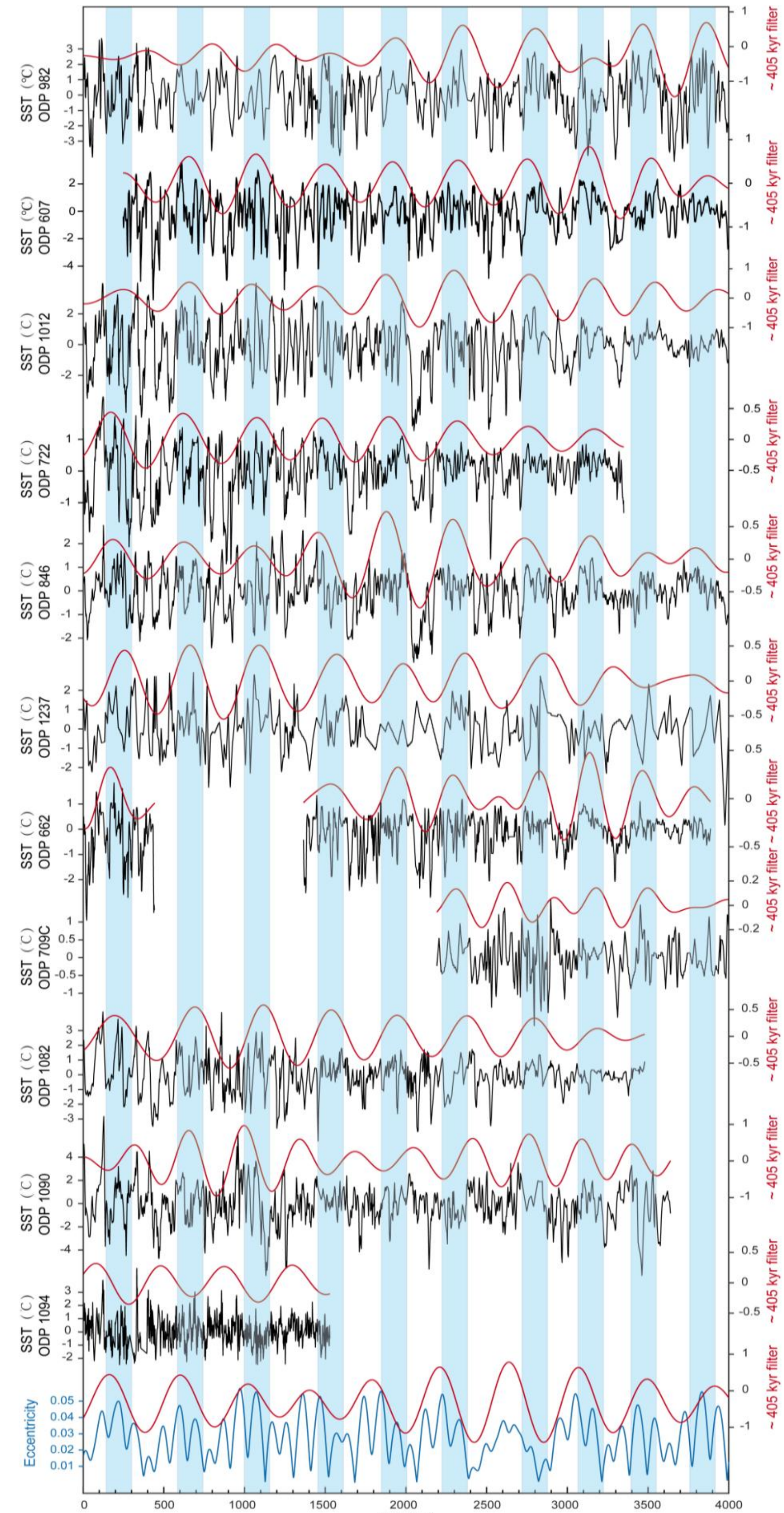


**Fig. S3 Detrended SST data for each site and their 405 kyr filter (0.0024±0.0006 cycles/kyr).** All SST data were detrended by removing 35% of the long trend using the LOESS functions.

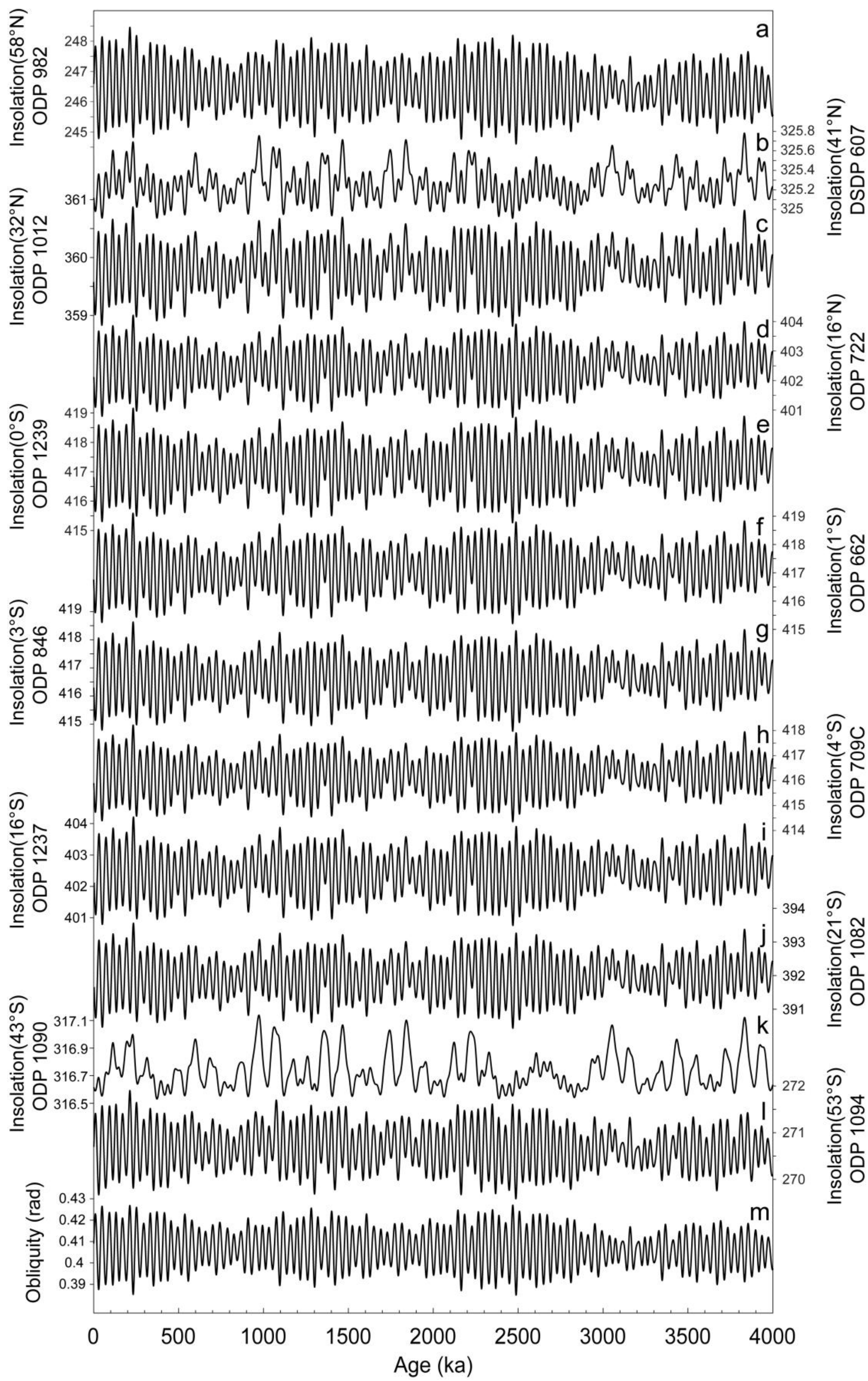


**Fig. S4. Annual mean insolation at the latitude of the ODP sites (a-l; Laskar et al., 2004) and the La2004 obliquity solution (m; Laskar et al., 2004).**

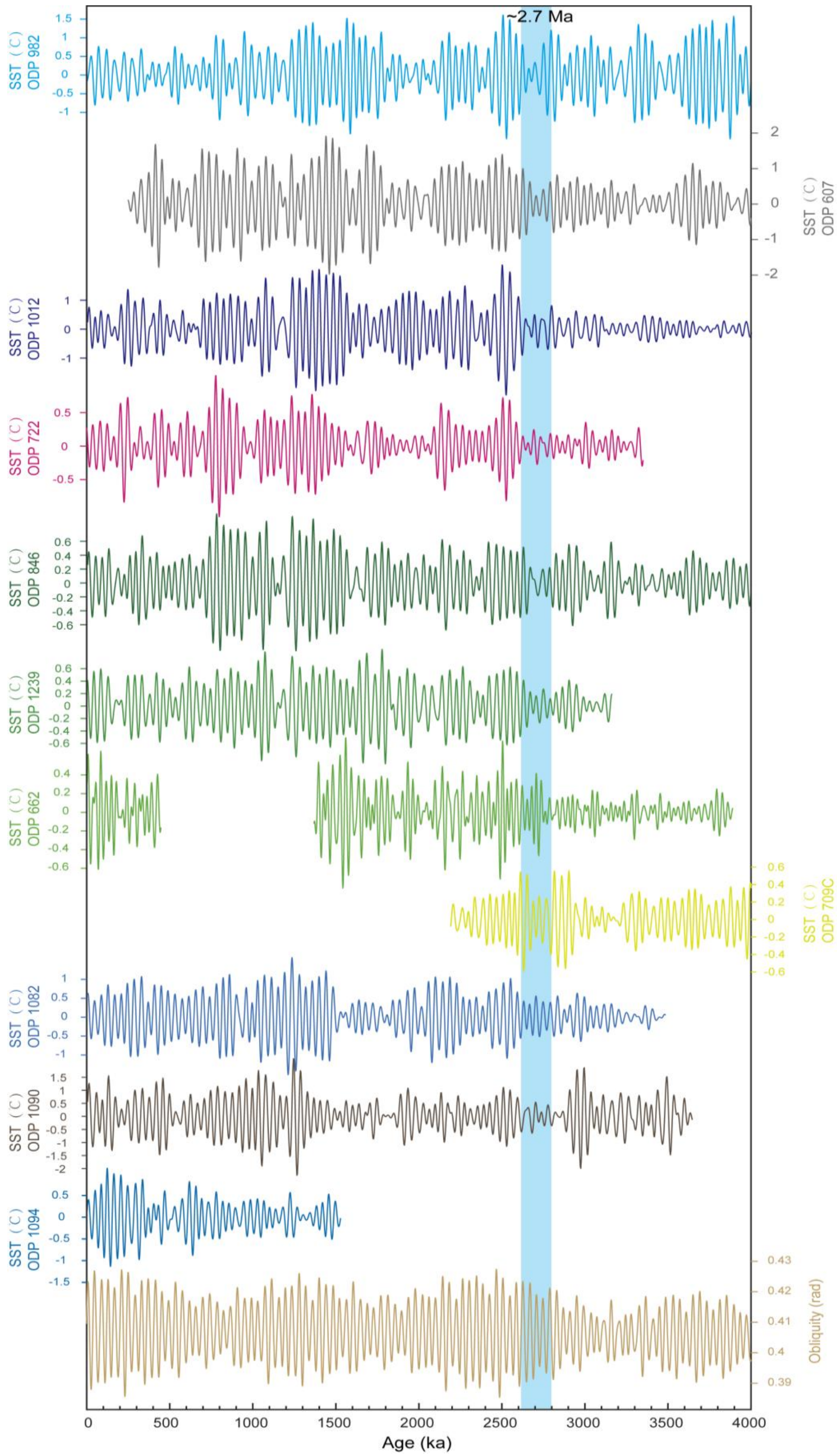


**Fig. S5 Filtered 41 kyr obliquity signals in SST at each site (Gaussian bandpass filters, filter passband: 0.024±0.006).** The blue shaded bar is centered at ~2.7 Ma; note the increase in obliquity amplitude of the SST records at northern hemisphere sites ODP 982, 607, 1012 and 772 at around this time.

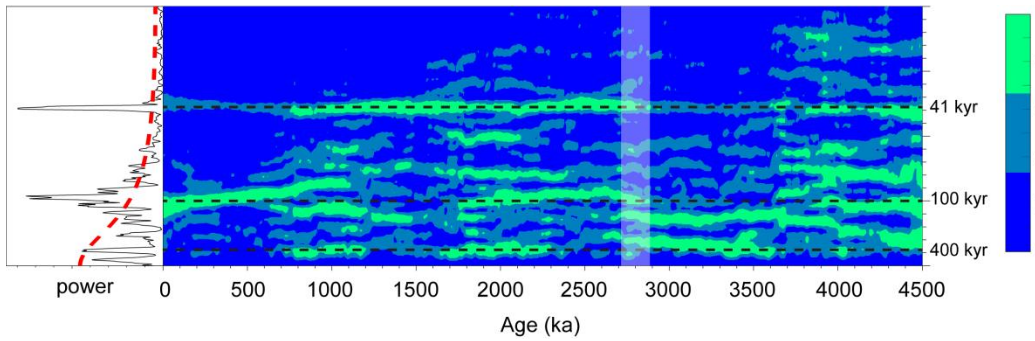


**Fig. S6. Evolutionary spectra of global sea surface temperature (SST stack) for 0-4.5 Ma (SST stack data from Clark et al., 2024).** The red dotted line in the left-hand panel indicates the 95% confidence level; ticks on the power x-axis of that panel indicate strength of the periodic signal (increasing from right to left). The white shaded band indicates the enhancement of the obliquity signal at ~2.7 Ma.

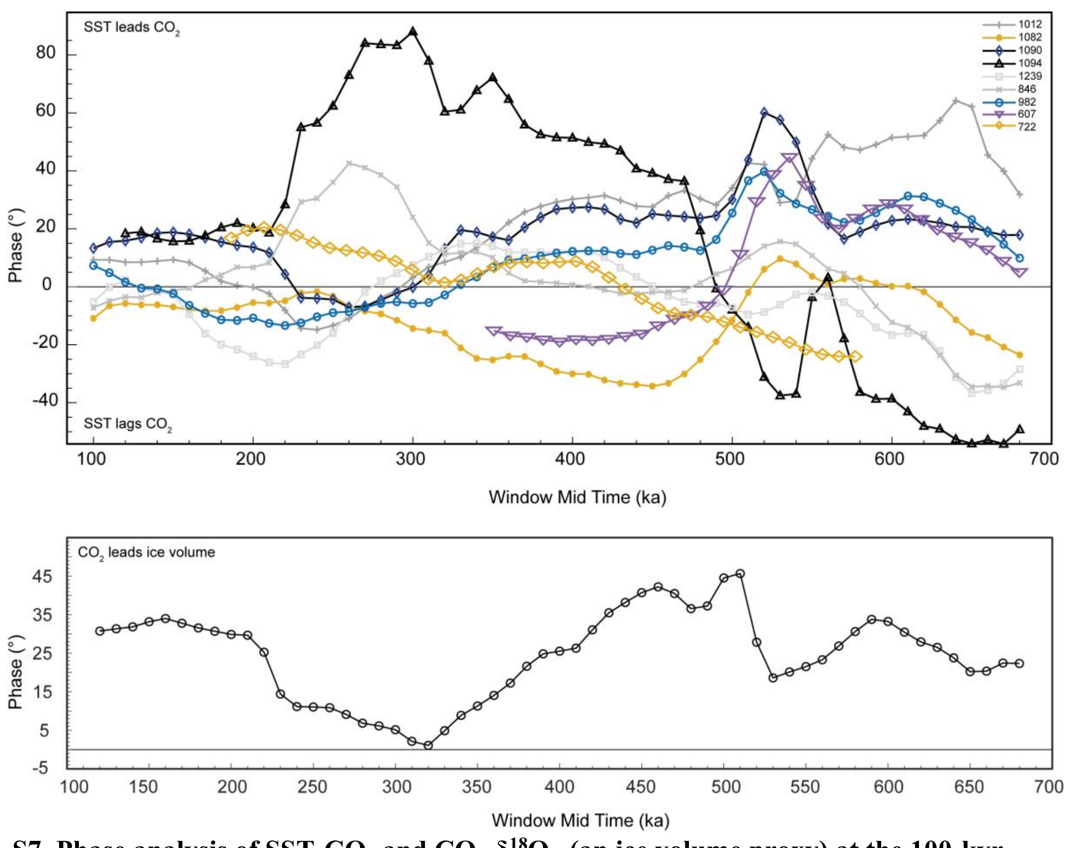


**Fig. S7. Phase analysis of SST-$CO_2$ and $CO_2$-$\delta^{18}O_w$ (an ice volume proxy) at the 100-kyr eccentricity scale over the past 800 kyr.** A typical confidence interval in the phase assessment is ±6°. Atmospheric $CO_2$ concentrations are from Antarctic ice cores (0-22 kyr BP: Monnin et al. 2001; 22-393 kyr BP: Petit et al. 1999; Pépin et al. 2001; Raynaud et al. 2005; 393-664 kyr BP: Siegenthaler et al. 2005a, b; 664-800 kyr BP: Lüthi et al., 2010). The $\delta^{18}O_w$ data are from Rohling et al. (2021).

**Table S1: Description of the ODP sites used in this study**

| ODP/ DSDP Sites | Location | Calibration | Resolution | Age model | Age uncertainty | Reference |
|---|---|---|---|---|---|---|
| 982 | North Atlantic (58°N, 16°W) | Müller et al. (1998) | ~3 kyr (2.5-1.75 Ma); 10 kyr (1.25-0.4 Ma) | Tuning to LR04 | - | Lawrence et al. (2009) |
| 607 | North Atlantic (41°N, 33°W) | Müller et al. (1998) | 3-4 kyr | Tuning to LR04 | - | Lawrence et al. (2010) |
| 1012 | North Pacific (32°17’N,118° 24’W) | Müller et al. (1998) | ~3 kyr | 5 biostratigraphic control points; Tuning to SST of ODP 846 (The age model for Site 846 was derived from LR04) | - | Brierley et al. (2009) |
| 722 | Arabian Sea (16.6°N, 59.8°W) | Müller et al. (1998) | ~2 kyr | Tuning to LR04 | - | Herbert et al. (2010) |
| 1239 | Eastern equatorial Pacific (0°40.32’S, 82°4.86’W) | Müller et al. (1998) | 2-4 kyr | Tuning to LR04 (3.2 to 2.7 Ma); Tuning to SST of ODP 846 (2.7-0.5 Ma) | <10 kyr | Etourneau et al. (2010) |
| 846 | Eastern equatorial Pacific (3°S, 91°W) | Müller et al. (1998) | ~3 kyr | Tuning to LR04 | <10 kyr | Liu and Herbert, (2004); Lawrence et al. (2006) |
| 1237 | Peru Margin (16°S, 76°23’W) | Müller et al. (1998) | 14 kyr | Biostratigraphic ages | - | Dekens et al. (2007) |
| 662 | Equatorial Atlantic (1°S, 12°W) | Müller et al. (1998) | 2.4 kyr | Tuning to LR04 | - | Herbert et al. (2010) |
| 709C | Indian Ocean (3°54.9’S, 60°33.1’E) | Dekens et al. (2002) | 3-10 kyr | Tuning to Site 806 (The age model for Site 806 was derived from LR04) | <10 kyr | Karas et al. (2011) |
| 1082 | South Atlantic (21°5’S, 11°49’E) | Müller et al. (1998) | ~3 kyr | Paleomagnetic; Tuning to LR04 | - | Etourneau et al. (2009) |
| 1090 | Subantarctic (42°54.5’S, 8°54.0’E) | Müller et al. (1998) | 2-3 kyr | Tuning to LR04 (2.9-0 Ma); biostratigraphy (3.65-2.9 Ma) | - | Martínez-Garcia et al. (2010) |

| | | | | | | |
|---|---|---|---|---|---|---|
| 1094 | Antarctic (53.2°S, 5.1°E) | Vázquez Riveiros et al. (2016) | ~1 kyr | Tuning to LR04 | - | Hasenfratz et al. (2019) |

**Text S1: Recurrence analysis**

Recurrence analysis (RA) is used to identify transitions between different types of dynamics within a time series (Marwan et al., 2007; Westerhold et al., 2020). Recurrence plots (RP) are matrix plots that visualize a fundamental property of dynamical systems – namely, when a system ‘repeats’ itself, returning to a previous state (Marwan et al., 2007). A value 1 at column i and row j indicates that the state at time i recurs at time j. It identifies the times j at which a system ‘repeats’ itself and recurs to a previous state $x_i$:

$$R_{i,j}(\in) = \Theta\left(\in - \left\|\vec{x_i} - \vec{x_j}\right\|\right) \quad i, j = 1, \ldots N \qquad \text{(1) (Marwan et al., 2007)}$$

Here, Θ is the Heaviside function, Θ(y)=1 if y≥0 and 0 otherwise (Marwan et al., 2007). ∈ is a recurrence threshold, $\|\vec{x_i} - \vec{x_j}\|$ represents the Euclidean distance between two states $x_i$ and $x_j$ in the phase space, and N is the time series length. This method is well-suited to capture regime changes, as such an extreme event would result in a sudden reduction in the number of recurring events (Marwan et al., 2007). The recurrence plot is a binary matrix plot, with diagonal structures paralleling the main diagonal, indicating sections of the trajectory with locally similar paths. This is a measure of the amount of predictability within the system, as stochastic or chaotic systems result in none or only short diagonals (Marwan et al., 2007; Westerhold et al., 2020). In our study, if climate dynamics have similar patterns, they will show up as darker areas in the Recurrence plot; if they have no common dynamics, the plot will remain white.

A recurrence is defined by the pairwise comparison of all values in the time series, whether their distance is smaller than a predefined threshold. The threshold is selected in a way that compute Recurrence quantification analysis (RQA) for an increasing threshold and to look for a region where RQA measures change slowly (Schinkel et al., 2008). The graphical rendering of the RP can be used to get a first order visual impression of the type of dynamics and to identify changes of the dynamics. RP is a powerful tool to reveal nontrivial dynamical features that can effectively capture regime changes (Marwan et al., 2007; Eroglu et al., 2016). We conducted RA in Matlab’s CRP Toolbox (Marwan, 2020) in the time domain. Analysis was performed on non-detrended proxy records (Figure 5c). An RP contains a number of interesting and important small-scale features, such as single points or diagonal lines (Marwan et al., 2007). A dominance of single points indicates stochastic processes. The more diagonal lines exist with respect to single points, the more deterministic or predictable the process would be (Marwan et al., 2007).